ORIGINAL PAPER

Damage analysis of retired typhoons in mainland China from 2009 to 2019

Chengcheng Wan[1] · Yafei Yan[1] · Liucheng Shen[1] · Jianli Liu[2] · Xiaoxia Lai[1] · Wei Qian[1] · Juan Nie[3] · Jiahong Wen[1]

Abstract

Typhoon catastrophes can seriously threaten national and regional security and development. How to quantitatively portray the spatiotemporal characteristics and the causes of typhoon catastrophe losses will be an important subject of scientific research in terms of disaster risk reduction. In this study, the overall characteristics, spatial patterns, and main influencing factors of the losses caused by retired typhoons landing in mainland China from 2009 to 2019 were investigated, through the usage of improved typhoon disaster index (G-index), spatial autocorrelation, and cold/hotspots analysis methods. The results showed that 18 retired typhoons affected 17 provinces in China from 2009 to 2019, among which the areas affected by minor, moderate, severe, and extremely severe disasters accounted for 38.02%, 44.16%, 13.84%, and 4.32%, respectively. The disaster has strong spatial clustering, and the hotspots based on the G index are the key areas to be concerned about prevention and mitigation against typhoon mega-disasters. Furthermore, the effects of exposed population, maximum wind speed, and maximum accumulative process precipitation on typhoon disaster losses were positively correlated, while the effects of exposed GDP (Gross Domestic Product) on disaster losses are weakly negatively correlated. This study identified the hotspots of typhoon catastrophes and underlined the efforts to formulate effective disaster risk reduction and build resilience.

Keywords Catastrophe · Retired typhoon · Typhoon disaster index · Spatiotemporal distribution · China

✉ Juan Nie
  niejuan@ndrcc.org.cn

✉ Jiahong Wen
  jhwen@shnu.edu.cn

1 School of Environment and Geographical Sciences, Shanghai Normal University, Shanghai 200234, China

2 School of Science, Technology and Engineering, University of the Sunshine Coast, Sunshine Coast, QLD 4556, Australia

3 National Disaster Reduction Center of China, Beijing 1000124, China

1 Introduction

Typhoon disaster that often causes huge casualties and property damage (Gao et al. 2014; Wang et al. 2021) is one of the most serious natural disasters in the world as well as in China (Schmidt et al. 2010; Zhang et al. 2017). For example, in 2013, typhoon Fitow caused direct economic losses of nearly US$5 billion in Ningbo, Zhejiang Province, China (Gu et al. 2018). Typhoon Meranti in 2016 was the strongest typhoon hitting Fujian Province since 1950, and caused direct economic losses of US$255 million and 18 deaths (Yang et al. 2018). Typhoon Mangkhut in 2018 exposed much of China and the Philippines to its strong winds and heavy precipitation, caused the collapse of more than 3400 houses and damaged 341,400 hectares of crops in Guangdong and Guangxi, China (Niu et al. 2020; Zhang et al. 2021). There are 18 retired typhoons (According to the World Typhoon Committee, a retired typhoon is defined as a catastrophic typhoon that causes particularly significant property damage or human casualties, its name is removed from the nomenclature, and the name is no longer used for other subsequent typhoons) that caused significant damage to China during 2009–2019 (Lei and Zhou 2012). Moreover, global warming may increase the frequency and intensity of typhoons in the northwest Pacific (Webster et al. 2005; Cheng-lin et al. 2016; Park et al. 2017; Nerem et al. 2018; Wu et al. 2018), while the population and economy in coastal areas in China are increasing dramatically (Corban et al. 2017). China's coastal areas are facing more severe typhoon disaster risks under rapid urbanization, economic growth, and climate change (Chen et al. 2017). Therefore, there is an urgent need to explore comprehensive study on typhoon catastrophe losses to improve disaster losses accounting, disaster forensics and risk modeling (De Groeve et al. 2013; Zuzak et al. 2021).

Previous studies on typhoon disaster loss were mainly focused on three aspects. First, typhoon loss models were developed to evaluate the spatiotemporal characteristics of typhoon disasters in Germany, Fujian Province, Ningbo city, and Hainan Province of China, respectively (Klawa and Ulbrich 2003; Zhu et al. 2017; Gu et al. 2018). Second, future loss trends caused by tropical cyclones were studied in the context of global climate change. Gettelman et al. (2018), Chen et al. (2018), and Cha et al. (2020) predicted increasing damage and impacts from future tropical cyclones based on global climate models. Third, assessing the damage and impact caused by individual extreme typhoon events as well as the influencing factors was focused. For example, Esteban et al. (2015) and Nakamura et al. (2016) analyzed the damage of retired typhoon Haiyan in 2013. Ding et al. (2020) revealed that the long residence time and high potential height were the main reasons for the huge losses caused by typhoon Lekima in 2019. However, previous studies are less comprehensive for a series of typhoon catastrophes on a certain timescale with significant socioeconomic impacts and losses, and the understanding of the overall characteristics of typhoon catastrophe losses, spatial patterns and their influencing factors is still insufficient. Therefore, this paper analyzes the catastrophe loss data of 18 retired typhoons in mainland China from 2009 to 2019 and explores the affected population, casualties, number of collapsed houses, affected crop area, direct economic loss and comprehensive disaster characteristics of retired typhoons that landed in mainland China from 2009 to 2019 by using improved typhoon disaster index (G index), spatial autocorrelation and cold/hotspots analysis methods. Moreover, the influencing factors of disaster losses were identified, using the Ordinary Least Squares (OLS) model.

The following parts of this study contain three sections. Section 2 provides a brief description on the datasets and methodology used in this study. The temporal and spatial

characteristics of retired typhoons, their losses and influencing factors are presented in Sect. 3. Section 4 provides major conclusions of the study.

2 Data and methods

2.1 Data

The datasets used in this study mainly include typhoon disaster damage data, basic information of retired typhoons, and the corresponding socioeconomic data.

Damage data include the number of people affected, houses collapsed, casualties, crop area affected and direct economic losses for the 18 retired typhoons that made landfall in China from 2009 to 2019. These data cover 1019 counties and districts in 17 provinces (Jilin, Liaoning, Hebei, Shandong, Henan, Jiangsu, Anhui, Shanghai, Zhejiang, Jiangxi, Fujian, Hunan, Guizhou, Yunnan, Guangxi, Guangdong, and Hainan provinces) of China. Damage data are obtained from the Yearbook of Meteorological Disasters in China (https://data.cnki.net/statisticalData.), historical meteorological disaster census information, and disaster statistics provided by relevant departments. Basic information about the 18 retired typhoons is shown in Table 1. The best track data of the retired typhoons were obtained from Typhoon Online (https://www.typhoon.org.cn) (Ying et al. 2014; Lu et al. 2021). Among them, typhoon intensity is determined according to the China Meteorological Administration's tropical cyclone classification standard (GBT 19201-2006). Typhoons are classified into six classes (tropical depression, tropical storm, strong tropical storm, typhoon, strong typhoon, and super typhoon) based on the maximum average wind speed near the bottom center. In this paper, typhoon 10 m wind field data and precipitation data were available from EAR5 reanalysis dataset with a temporal resolution of 1 h and spatial resolution of $0.25° \times 0.25°$ (https://cds.climate.copernicus.eu).

Socioeconomic data include population and GDP grid data in the year of 2015. Population data with a spatial resolution of 100 m × 100 m (http://www.worldpop.org) were generated by employing methods of random forest and dasymetric mapping to spatialize the district and county census data into grid data. 2015 GDP grid data were obtained from the Earth System Science Data Sharing Platform (http://www.geodata.cn). Based on land use data, the district and county level GDP statistics are interpolated to produce the GDP kilometer grid data.

The basic data include the standard base map of the standard map service system of the National Bureau of Surveying, Mapping, and Geographic Information. To eliminate the influence of prices, this paper introduces the fixed-base price ratio coefficient (this paper takes 2015 as the base year), which is obtained by converting the 1978 fixed-base price coefficient provided by the National Bureau of Statistics (http://data.stats.gov.cn).

2.2 Methods

2.2.1 Typhoon disaster index

To comprehensively assess the retired typhoon damage, this paper improves the Typhoon Disaster Index (ATDI) (Meng et al. 2007; Lei et al. 2009) by integrating the indicator of the affected population to form a new typhoon disaster index I_G (called G index). I_G is the sum of each damage index caused by a typhoon to a county. For comparison purposes, we

Table 1 Basic characteristics of retired typhoons during 2009–2019

Serial number	Year	Month	Retired typhoon name	Typhoon intensity	Maximum wind speed (unit: m/s)	Lowest pressure in center (unit: hP)	Affected provinces
1	2009	10	Parma	Super typhoon	55	935	Hainan, Guangdong
2	2009	9	Ketsana	Typhoon	40	960	Hainan
3	2009	8	Morakot	Typhoon	40	950	Fujian, Jiangxi, Anhui, Jiangsu,
4	2010	9	Fanapi	Super typhoon	52	935	Guangdong, Guangxi, Fujian,
5	2012	7	Vicente	Typhoon	45	960	Guangdong, Fujian, Guangxi
6	2013	11	Haiyan	Strong typhoon	78	890	Hainan, Guangdong, Guangxi
7	2013	10	Fitow	Strong typhoon	45	945	Fujian, Zhejiang, Shanghai, Jiangsu
8	2013	8	Utor	Typhoon	60	925	Hainan, Guangdong, Guangxi, Hunan
9	2014	7	Rammasun	Super typhoon	72	888	Hainan, Guangdong, Guangxi, Yunnan
10	2015	10	Mujigae	Super typhoon	52	935	Hainan, Guangdong, Guangxi,
11	2015	8	Soudelor	Super typhoon	68	905	Fujian, Zhejiang, Jiangxi, Anhui, Jiangsu
12	2016	10	Haima	Super typhoon	68	905	Guangdong, Fujian, Jiangsu
13	2016	9	Meranti	Super typhoon	75	890	Fujian, Zhejiang, Jiangxi, Shanghai, Jiangsu
14	2016	10	Sarika	Super typhoon	55	935	Hainan, Guangdong, Guangxi,
15	2017	8	Hato	Strong typhoon	52	935	Guangdong, Fujian, Guangxi, Yunnan, Guizhou
16	2018	9	Mangkhut	Super typhoon	65	910	Hainan, Guangdong, Guizhou, Yunnan, Hunan
17	2018	8	Rumbia	Severe tropical storm	25	982	Zhejiang, Shanghai, Anhui, Jiangsu, Henan, Shandong, Hebei, Liaoning
18	2019	8	Lekima	Super typhoon	62	915	Fujian, Zhejiang, Anhui, Shanghai, Jiangsu, Shandong, Hebei, Jilin, Liaoning

also normalized the I_G (in the range 0–1). In the time series, we accumulate normalized I_G and calculate the I_Gs for different years and for each retired typhoon, respectively. In the spatial distribution, we summed the I_Gs of all typhoons for each county or district to obtain a spatial pattern of the disaster loss index. The higher the I_G, the higher the severity of disaster losses. The formula of the typhoon disaster index I_G (G index, hereafter) is expressed as follows:

$$I_G = I_p + I_d + I_h + I_e + I_m \tag{1}$$

Among them, I_p is the normalized affected population index; I_d, casualties index; I_h, affected crop area index; I_e, collapsed house index; I_m, direct economic loss index: The detailed formulas of these parameters are as follows:

$$I_p = \begin{cases} \log\ p - 2 & p \geq 10000 \text{ persons} \\ \frac{p}{10000} & p < 10000 \text{ persons} \end{cases} \tag{2}$$

$$I_d = \begin{cases} \log\ d - 2 & d \geq 100 \text{ persons} \\ \frac{d}{100} & d < 100 \text{ persons} \end{cases} \tag{3}$$

$$I_h = \begin{cases} \log\ (15 \times h) - 2 & h \geq 66.67 \text{ hm}^2 \\ \frac{15 \times h}{1000} & h < 66.67 \text{ hm}^2 \end{cases} \tag{4}$$

$$I_e = \begin{cases} \log\ e - 2 & e \geq 10000 \text{ rooms} \\ \frac{e}{10000} & e < 10000 \text{ rooms} \end{cases} \tag{5}$$

$$I_m = \begin{cases} \log\ m & m \geq \text{US\$} \frac{10}{6.2272} \text{ billion} \\ \frac{m}{10} & m < \text{US\$} \frac{10}{6.2272} \text{ billion} \end{cases} \tag{6}$$

In these formulas, p is affected population (unit: persons); d, number of casualties (unit: persons); h, affected crop area (unit: hm^2); e, number of collapsed houses (unit: rooms); m, direct economic loss (unit: billion). To eliminate the influence of price, the fixed-base index is introduced. The calculation for fixed-based index economic loss is as follows:

$$m = m_0 \cdot \beta \tag{7}$$

where m_0 is the direct economic loss of the current year, β, fixed-base index, and 2015 was taken as the base year in this study. The purpose of emending the economic losses in every year according to the base year is to eliminate price fluctuations and make the economic losses in different years comparable (Chen et al. 2009).

2.2.2 Disaster loss classification

Based on the G-index value, the affected areas were classified into different damage levels through the orderly sample clustering analysis (optimal segmentation method). The method requires that the samples are arranged in a certain order and that the classification is not disordered, i.e., the samples in the same class must be adjacent to each other (Zhi et al. 2019; Guo et al. 2020). In essence, some division points are found

that divide the ordered sample into several subsegments, each of which is considered as a class. One basis for finding the optimal division points is usually to minimize the variation between samples within each segment and to make a greater variation between samples within each segment. Using $B(n, k)$, for representing n ordered samples $\{\times 1, \times 2, \ldots, xn\}$ into k classes, this segmentation can be expressed as follows:

$$
\begin{aligned}
P1 &= \{i_1, \ i_1 + 1 \ldots i_2 - 1\}, \\
P2 &= \{i_2, \ i_2 + 1 \ldots i_3 - 1\}, \\
&\ldots \ldots \ldots \\
Pk &= \{i_k, \ i_k + 1 \ldots n\}.
\end{aligned}
\tag{8}
$$

2.2.3 Spatial pattern analysis

This paper explores the spatial distribution patterns of typhoon catastrophes through the spatial pattern analysis method. It mainly includes two types of autocorrelation analysis: global and local. The global autocorrelation method was used to analyze the spatial clustering state of typhoon disasters, while the local autocorrelation method was used to identify and locate the hotspots areas with severe typhoon impacts.

The global autocorrelation index, Moran's I, can be calculated to reveal the spatial distribution of space relationship (Anselin et al. 2010). The formula is as follows:

$$
I = \frac{n \sum_{i=1}^{n} \sum_{j=1}^{n} w_{ij} (x_i - \bar{x})(x_j - \bar{x})}{\sum_{i=1}^{n} \sum_{j=1}^{n} w_{ij} \sum_{i=1}^{n} (x_i - \bar{x})^2} = \frac{\sum_{i=1}^{n} \sum_{j \neq 1}^{n} w_{ij} (x_i - \bar{x})(x_j - \bar{x})}{s^2 \sum_{i=1}^{n} \sum_{j \neq 1}^{n} w_{ij}}
\tag{9}
$$

$$
s^2 = \frac{1}{n} \sum_{j} (x_i - \bar{x})^2 \quad \bar{x} = \frac{1}{n} \sum_{i=1}^{n} x_i
\tag{10}
$$

where n is the number of areas affected by the retired typhoon; x_i, G-index of county i, x_j, take point j as the center, and the G index of its adjacent counties; and w_{ij}, adjacent matrix standardized by the columns. The value of Moran's I is between -1 and 1. If I is greater than 0, it indicates a positive spatial correlation and the spatial entities are clustered; conversely, if I is less than 0, then it indicates a negative spatial correlation and the spatial entities are dispersed.

To identify the hotspots that are severely affected by the retired typhoons, the local autocorrelation method, Getis-Ord Gi*, was used to identify the spatial clusters of losses caused by the retired typhoon disasters that made landfall in China during 2009–2019. The Getis-Ord Gi* is expressed as follows:

$$
G_i^* = \frac{\sum_{j=1}^{n} w_{ij}(d) x_j}{\sum_{j=1}^{n} x_i}
\tag{11}
$$

where x_i is the attribute value of element j; w_{ij} is the spatial weight between elements i and j; n, the total number of elements.

2.2.4 Analysis of influencing factors

The Ordinary Least Square (OLS) model was used to analyze the attributing factors to the losses of typhoon disasters. Based on the experience of previous scholars and the availability of data (Yin et al. 2013; Li et al. 2016; Liu and Xu 2020), seven factors were selected to analyze influencing factors in this study, including exposed population, exposed GDP, tertiary industry share, number of hospital beds, arable land area, maximum wind speed, and maximum cumulative process precipitation.

For the maximum wind speed and precipitation, the 10 m wind speed field data and precipitation data were converted into gridded data, and the maximum wind speed and maximum cumulative process precipitation for each municipality were extracted for multiple typhoons. Finally, the maximum wind speed and maximum cumulative process precipitation for each affected city were extracted by kriging interpolation into raster data and then using the zonal statistics function. The seven factors were all normalized with the following equations (Shao et al. 2020; Ahmad et al. 2021).

$$A = \frac{x_i - \min_{1 \le i \le n} \{x_j\}}{\max_{1 \le i \le n} \{x_j\} - \min_{1 \le i \le n} \{x_j\}} \tag{12}$$

Seven factors were subjected to the OLS model for calculation and were required to pass a test of $P < 0.01$. VIF (variance inflation factor) < 7.5. Factors that do not pass will be excluded. The VIF is used to test for global multicollinearity, where the larger the value the more severe the collinearity and the more likely the data are to be redundant. The threshold value for VIF is usually set at 7.5 in OLS models (Ahmad et al. 2021). The OLS model aims to explore the regression of the independent variable on the dependent variable within the overall region:

$$y_i = \beta + \sum_{k=1}^{n} \beta_k x_{ik} + \varepsilon_i \tag{13}$$

In the formula, y_i is the dependent variable (disaster index G) at position i in space; β, the spatial intercepts of squares; β_k, the regression coefficient of the "kth" independent variable (driver); x_{ik}, the value of the "kth" independent variable (driver) taken at position i in space, and ε_i, the residual of the algorithm. The analytical framework for screening the influencing factors is shown in Fig. 1.

3 Results

3.1 Characteristics of retired typhoons in mainland China from 2009 to 2019

According to China's Tropical Cyclone Rating Standard (GB/T19201-2006), 11 out of 18 typhoons retired during 2009–2019 were super typhoons (Table 1). Among them, Typhoon Haiyan in 2013 had the maximum wind speed (78 m/s) and the minimum central pressure (890 hPa). 18 retired typhoons affected 17 provinces in China, and the most frequently affected province was Guangdong Province, with 11 times (Fig. 2). About 126 million people were affected by the 18 retired typhoons during 2009–2019, with more than 20,000
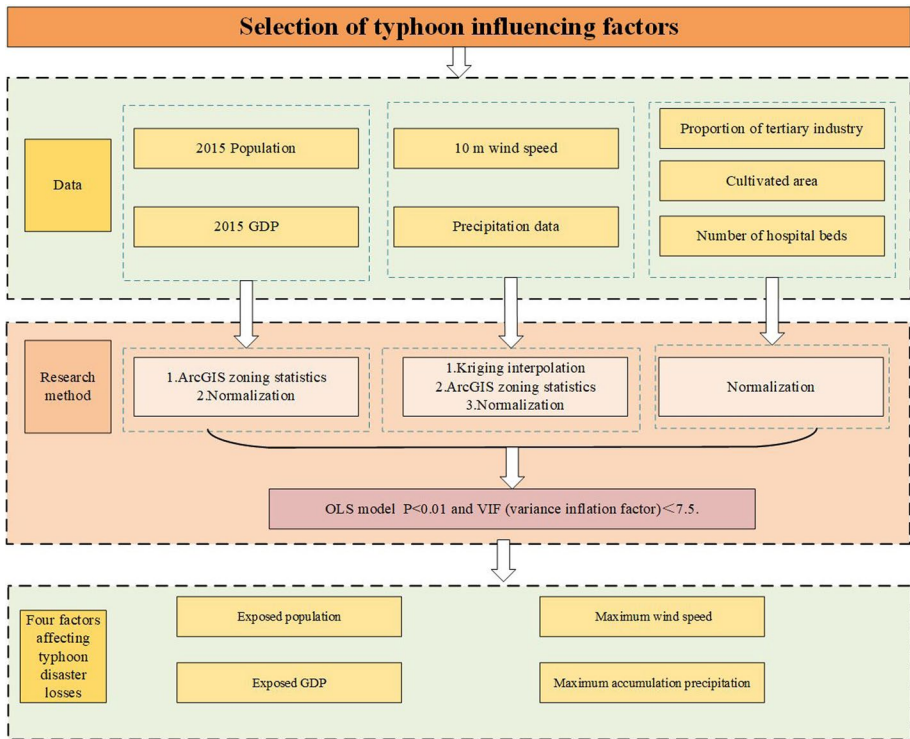
Fig.1 Analytical framework for influencing factor analysis

life casualties, around 230,000 houses collapsed, more than 10 million hectares of crops affected, and the US$75 billion direct economic losses (at 2015 baseline prices, eliminating the price increase factor).

The years with the highest number of retired typhoons were 2009, 2013 and 2016, with three retired typhoons in each year. In terms of the losses, the largest number of the affected population (about 30 million) and collapsed houses (70,000) happened in 2013; the largest number of casualties (14,000 people) was in 2009; the largest area of affected crops (2.35 million hectares) was in 2018; the most serious direct economic losses (more than the US$16.8 billion) occurred in 2019. Except for the year with the least collapsed houses (0.19 million houses) in 2017, the year with the least losses was 2012. The highest value of the combined disaster index (G) was 207.96 in 2013 as shown in Fig. 3, indicating that the most serious damage was caused by the impact of retired typhoons in 2013.

In terms of a single retired typhoon, typhoon Rumbia in 2018 affected the largest area of crops (more than 2 million hectares), and the largest number (more than 15 million) of people affected. Typhoon Lekima in 2019 caused the most serious direct economic losses (more than the US$8.627 billion). Typhoon Ketsana in 2009 caused the largest number of casualties (more than 7200 due mainly to injuries and illnesses). Typhoon Meranti in 2016 caused the largest number (18,000) of collapsed houses. In contrast, typhoon Haima in 2016 caused the fewest casualties (0). Typhoon Ketsana in 2009 caused the fewest affected population (1.4 million), affected crop areas (50,000 hectares), collapsed houses (0.22 million) and direct economic losses (the US$38 million). To further reveal the overall degree
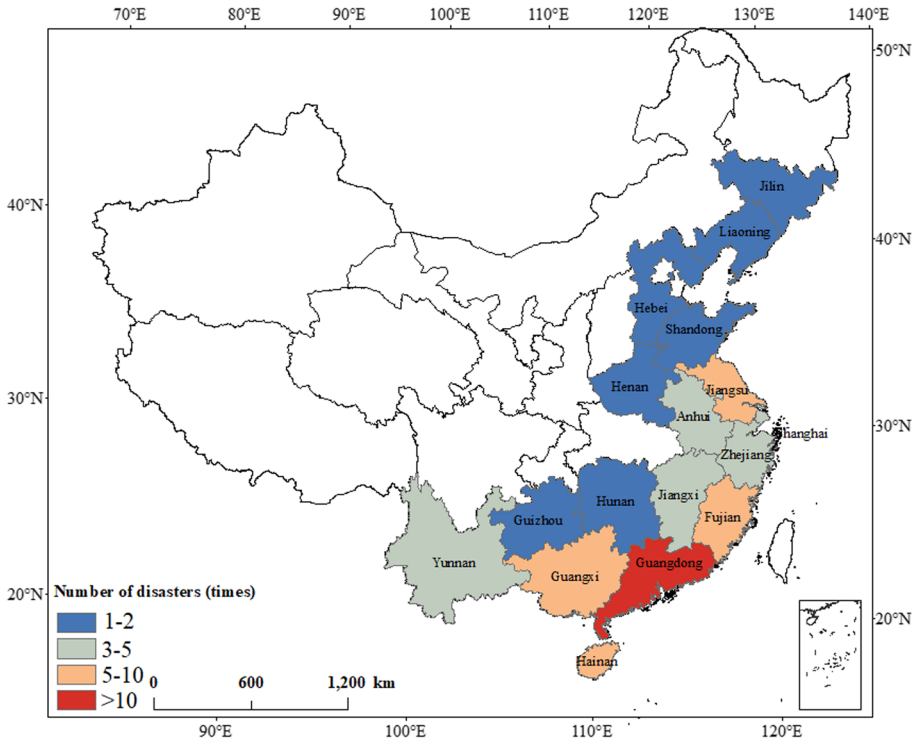
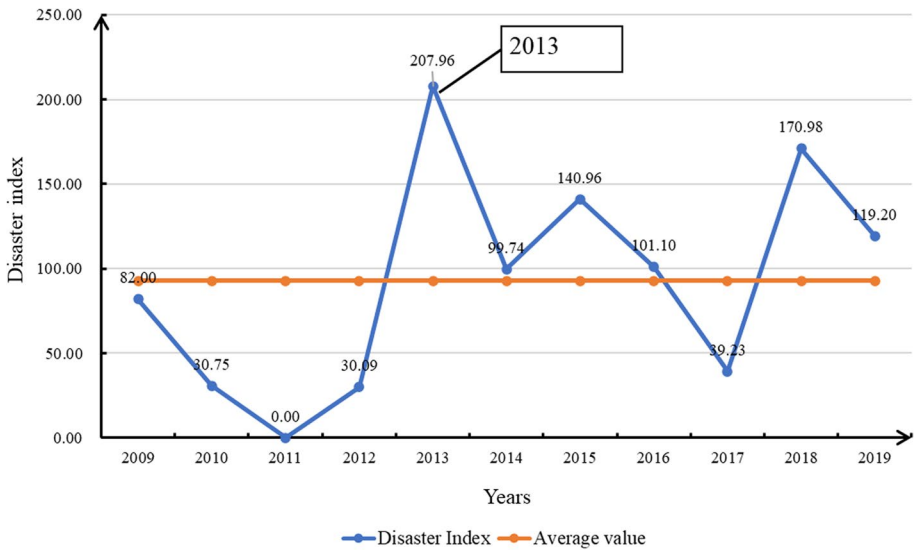**Fig. 2** Spatial distribution of the occurrence frequency of typhoon during 2009–2019

Fig. 3 Interannual variation of disaster index of retired typhoon during 2009–2019

of the disaster by G index, we found that typhoon Lekima in 2019 caused the most severe damage with the highest disaster index of 119.20, while typhoon Ketsana in 2009 caused the least damage with the smallest disaster index of 9.43 (Fig. 4).

3.2 Classification and spatial pattern of retired typhoon disaster losses

3.2.1 Spatial distribution of disaster losses

The spatial distribution of retired typhoon disaster losses in different affected regions was obtained by normalizing the affected population, casualty population, number of collapsed houses, affected area of crop and direct economic loss as well as spatial analysis of cold/ hotspots (Fig. 5).

During the period 2009–2019, the population affected by retired typhoons was mainly distributed in Hainan Province and the Leizhou Peninsula, as well as in the eastern part of Fujian, Zhejiang, and Jiangsu provinces (Fig. 5a). The average proportion of I_p in the I_G is up to 54%, indicating I_p is an essential component of I_G. Spatially, the minimum value of I_p for each county is 0, and the maximum value is 23.44. The maximum value is located in Wanning City, Hainan Province, which has the largest cumulative population affected (more than 1.4 million people). In terms of the individual typhoons, the maximum value of the I_p is 119.20 (Lekima) and the minimum value is 9.43 (Ketsana). The regions with high casualty population normative index were mainly concentrated in the coastal areas of Hainan Province, the eastern coastal areas of Zhejiang and Fujian Provinces (Fig. 5b). Among them, the highest casualty population normative index was 5.18 in Dongfang City, Hainan Province, with normative number of casualties (nearly 9000), due mainly to more than 6000 injured and sick people caused by Ketsana in 2009.

The areas with the most collapsed houses were mainly concentrated in the Leizhou Peninsula, the border of Guangxi and Guangdong provinces, the eastern parts of Zhejiang and Fujian Provinces, and the central parts of Shandong Province (Fig. 5c). Among them, the highest normalized index of collapsed houses was 2.35 in Wenchang City, Hainan Province, with the largest number of collapsed houses (more than 20,000). The regions with the largest area of crop were concentrated on the Leizhou Peninsula and its surrounding Guangdong and Guangxi Provinces, southern Liaoning Province and
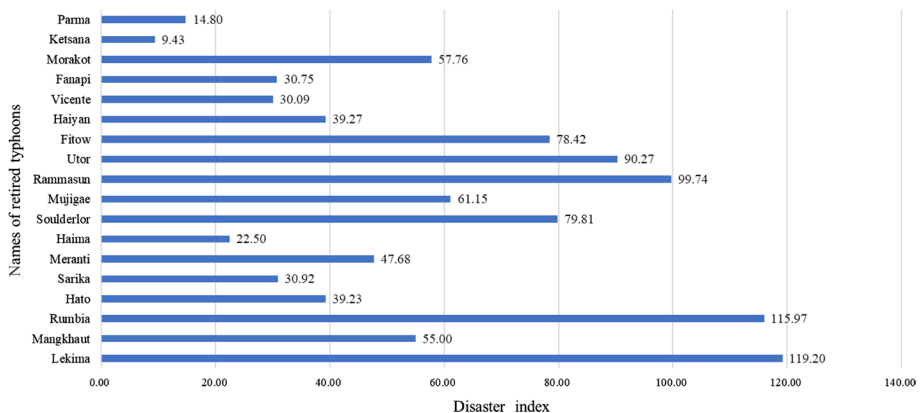

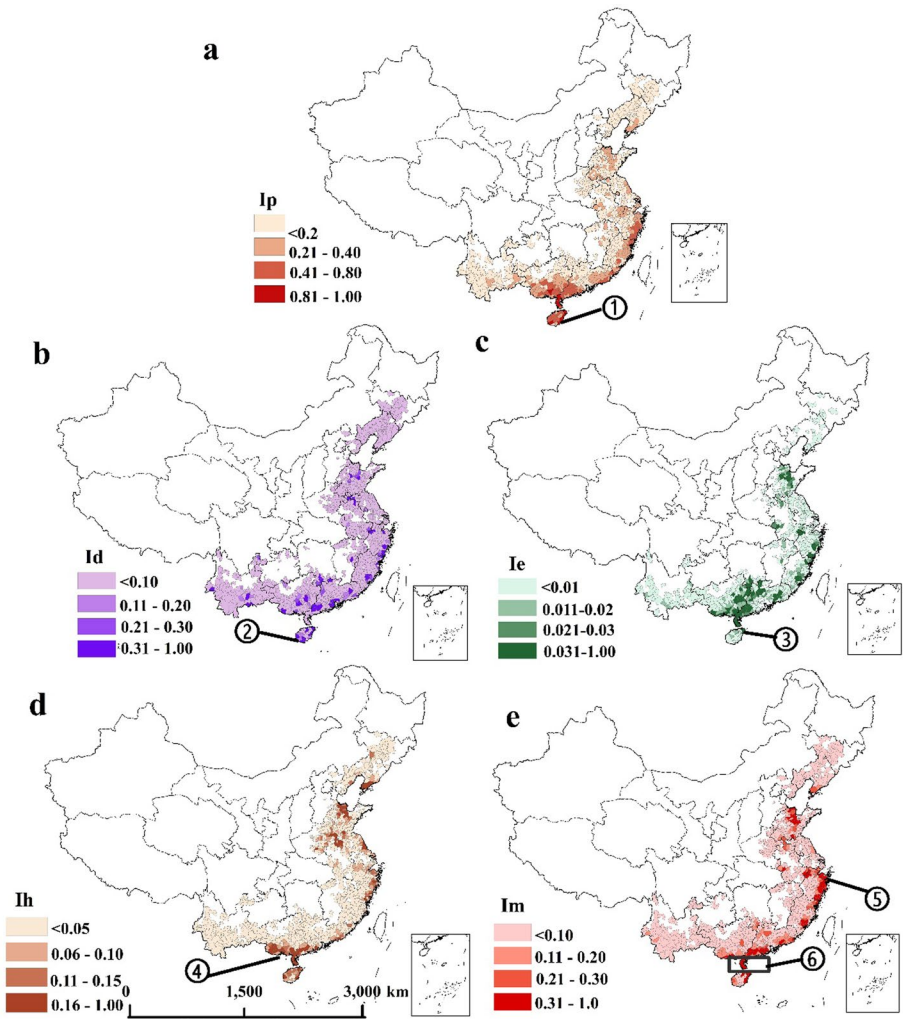**Fig. 4** Disaster index of the 18 retired typhoons during 2009–2019

Fig. 5 Spatial distribution of the standardized index of retired typhoon disaster in 2009–2019 **a** affected population, **b** casualties, **c** collapsed buildings, **d** affected area of crops, **e** direct economic loss; ① Wanning City, ② Dongfang City, ③ Wenchang City, ④ Shangsi County, ⑤ Linhai City, ⑥ Leizhou Peninsula

northern Shandong and Anhui provinces (Fig. 5d). In particular, Shangsi County in Guangdong Province has the highest index of crop disaster (2.6), with the affected crop area up to 230,000 ha. High values of direct economic losses were mainly distributed in northeastern Hainan Province, southwestern Guangdong Province, eastern Fujian and Zhejiang Provinces, and central Shandong Province (Fig. 5e). Among them, the highest normalized index was 3.63 in Linhai City, Zhejiang Province, and direct economic losses amounting to the US$1863 million.

Table 2 Disaster loss classification of retired typhoons during 2009–2019

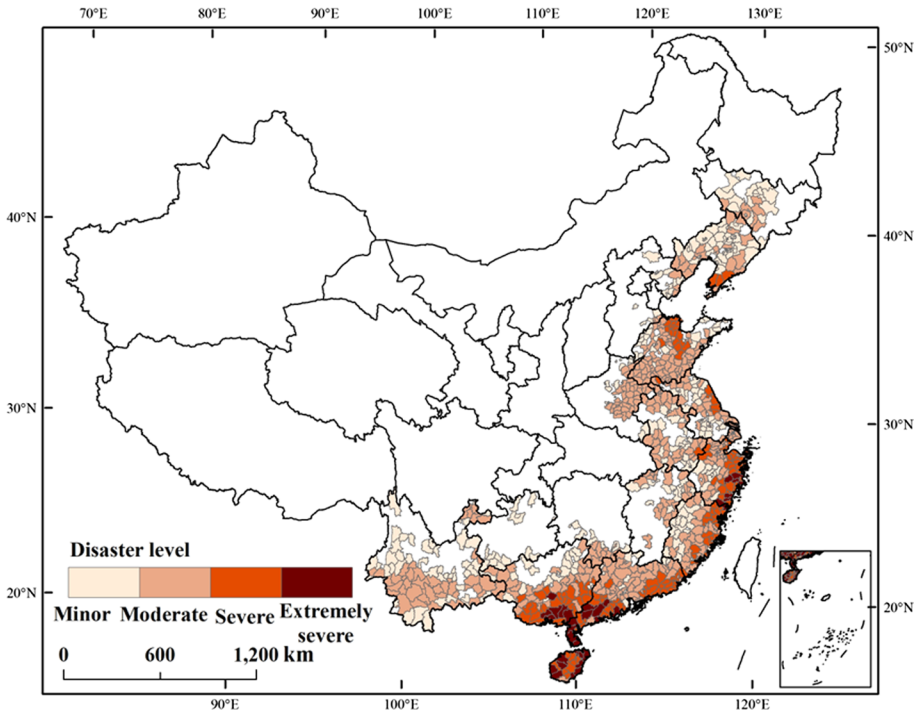| Disaster loss level	Minor	Moderate	Severe	Extremely severe
I_G	$I_G \leq 0.066$	$0.066 > I_G \leq 0.23$	$0.23 > I_G \leq 0.45$	$I_G > 0.45$

Fig. 6 Spatial distribution of classification of retired typhoon disaster loss in 2009–2019

3.2.2 Classification of disaster losses

The *G* index is a composite loss index made up of a combination of five disaster index (affected population, number of casualties, affected crop area, collapsed house, and direct economic loss). Because it is important to determine the spatial distribution of the disaster damage level in order to carry out services for typhoon prevention and mitigation. Therefore, this study classified four disaster levels (minor, moderate, severe and extremely severe) according to the ordered sample cluster analysis method (Table 2), and their spatial distribution is shown in Fig. 6. The results show that there were 384 counties and districts within minor loss level (accounting for 38.02% of the total affected areas). Four hundred fifty counties and districts (accounting for 44.16%) belonged to moderate loss. One hundred forty-one counties and districts (accounting for 13.84%) belonged to severe damage levels, while 44 counties and districts (4.32%) were hit by retired typhoons with extremely severe losses. The minor and moderate disaster losses are mainly located in the inland areas, while the severe and extremely severe disasters are concentrated in the eastern coastal areas (Fig. 6). In short, the disaster loss level showed a gradual decrease
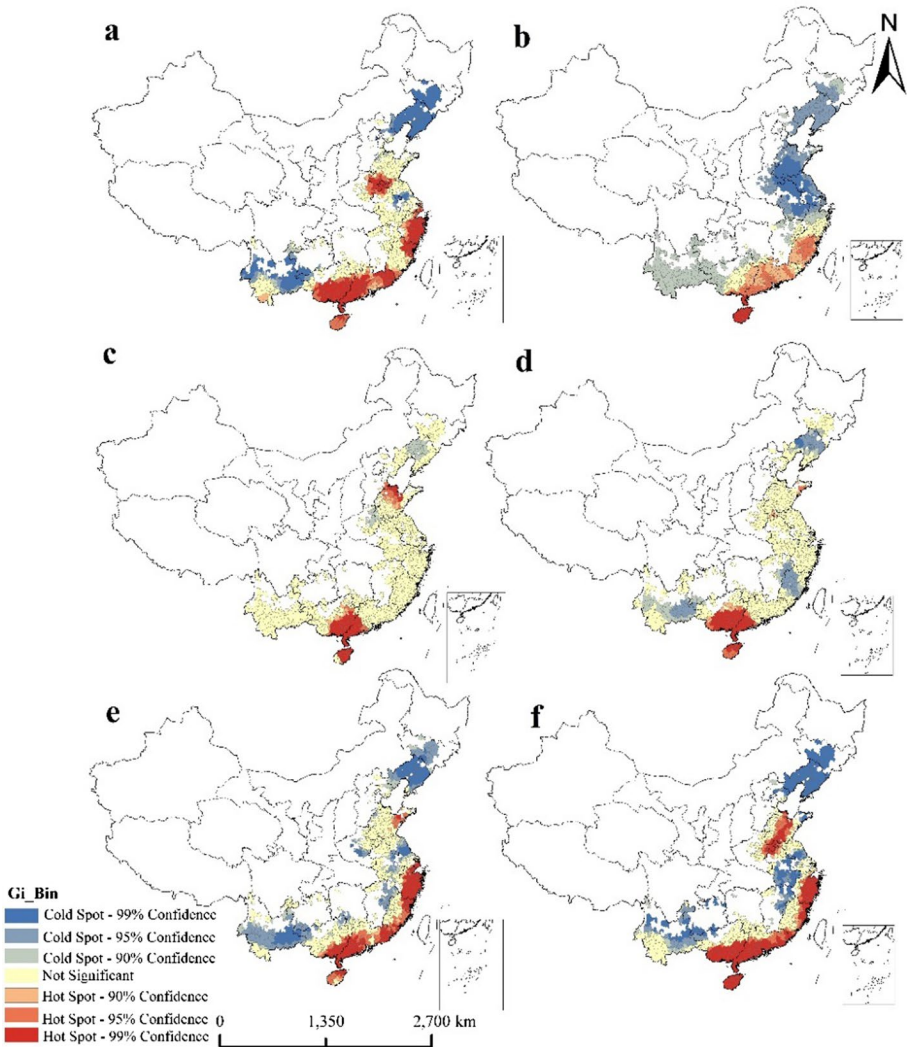
Fig. 7 The analysis of cold/hotspots of the disaster of retired typhoons in 2009–2019 **a** affected population, **b** casualties, **c** collapsed buildings, **d** affected area of crops, **e** direct economic loss, **f** index of G

from coastal to inland provinces, with the coastal areas being more severely affected by typhoons. This result is consistent with the results of the spatial distribution of the impact intensity of landfall typhoons analyzed (Wu et al. 2020).

3.2.3 Hotspots of the disaster situation

The value of Moran's I helps to further demonstrate the spatial pattern of typhoon disaster losses by considering spatial autocorrelation relationships. The Moran's I value of disaster index G in this study was positive (0.41) with 99% confidence level, indicating that the

retired typhoon disaster had strong spatial clustering. At the same time, the local autocorrelation Getis-Ord Gi* method was used to analyze the hotspots of five loss indicators and G index and their ratio to the total affected areas, so as to determine the spatial distribution of hotspots. The warmer the color of the spots in Fig. 7 indicates the more severity and concentration of the disasters, while the colder the color of the spots indicates the less impact of the disasters.

A total of 318 counties and districts with direct economic losses were hotspots, accounting for 31.21% of the total affected counties and districts. The hotspots were mainly distributed in the eastern coastal Provinces, including Hainan Province, Guangxi Province, Guangdong Province, Fujian Province, Zhejiang Province, and northern Shandong Province (Fig. 7e).

Figure 7f shows the cold/hotspots of the G index, indicating the overall spatial distribution characteristics of losses caused by the 18 retired typhoons. Two hundred seventy-eight counties and districts were hotspots, accounting for 27.28% of the total affected counties and districts. The hotspots were mainly distributed in Hainan Province, Guangdong Province, southern Guangxi Province, Zhejiang Province, and eastern Fujian Province. It suggested that these areas had a concentration of damage and are more vulnerable to typhoon disasters.

3.3 Influencing factors of retired typhoon losses

Establishing an objective and effective indicator system is an important way to analyze the causes of typhoon disaster losses. In this paper, through the OLS model, according to the principle of $P < 0.01$ and VIF (variance inflation factor) < 7.5, three influencing factors of tertiary industry share, total number of sickbeds and arable land area were excluded (Shao et al. 2020; Ahmad et al. 2021). Finally, the effects of four factors on the disaster index G are analyzed including the exposed population, the exposed GDP, the maximum wind speed, and the maximum accumulative precipitation. The degree of fit (R^2) is 0.4 and the results are well explanatory (Table 3).

Among the four influencing factors, the exposed GDP was negatively correlated with disaster loss. This may be higher GDP means higher exposure, but also higher economic development. Cities with higher levels of economic development have better infrastructure and resilience to disasters and better mitigation measures. As a result, there is a weak negative correlation between GDP and losses. Thus, the overall disaster loss may be relatively small. The exposed population, the maximum wind speed and the maximum precipitation had positive correlations with disaster loss, that is, the larger values of these factors, the more serious of the disaster loss. Among the four factors, the exposed population has the largest correlation coefficient (0.35) with the disaster losses,

Table 3 Main indicators of OLS regression model

Driving factors	Coefficient	Significance	VIF
Exposed population	0.35	$p < 0.01$	3.20
Exposed GDP	−0.25	$p < 0.01$	3.15
Maximum wind speed	0.22	$p < 0.01$	3.43
Maximum accumulative precipitation	0.13	$p < 0.01$	3.40

indicating that the exposed population may be an essential factor that is attributed to the losses of the retired typhoons during 2009–2019.

4 Conclusion

In this paper, we used the data of delisted typhoon losses in mainland China during 2009–2019 to classify the disaster levels by calculating the typhoon disaster index, explore the hotspot areas of typhoon mega-disasters by spatial pattern analysis, and analyze the influencing factors of typhoon losses by OLS model. The main conclusions are as follows:

(1) The 18 retired typhoons during 2009–2019 affected 17 provinces, and Guangdong Province suffered the most attacks (11 times). The areas with the most severe damage in terms of population affected, number of collapsed houses, casualties, crop damage and direct economic loss for the 18 retired typhoons were Wanning City, Wenchang City and Dongfang City in Hainan Province, Shangsi County in Guangxi Province and Linhai City in Zhejiang Province. And the disaster losses have a strong spatial clustering.

(2) Three hundred and eighty-four counties and districts are a minor disaster, accounting for 38.02% of the total affected area; 450 counties and districts are a moderate disaster, accounting for 44.16% of the total affected area; 141 counties and districts are a severe disaster (accounting for 13.84%); 44 counties and districts are an extremely severe disaster (accounting for 4.32%). The levels of disaster losses decrease from coast to inland in space, and the hotspots of typhoon losses are mainly concentrated in coastal provinces. Hainan Province, southern Guangxi Province, Guangdong Province, Fujian Province and eastern Zhejiang Province were the hotspots in terms of disaster losses.

(3) Among the four influencing factors, i.e., exposed population, exposed GDP, maximum wind speed and maximum accumulative precipitation, three are positively correlated, except for exposed GDP which has a weak negative correlation with disaster losses. Among them, the correlation coefficient of the exposed population on disaster losses was the largest at 0.35, indicating the exposed population having the largest influence on disaster losses among the four factors. However, this study presents a preliminary analysis of the loss influencing factors of 18 retired typhoons in mainland China from 2009 to 2019 using the OLS model, and future studies are needed to further explore the typhoon hazard, exposure and vulnerability and their roles in catastrophic typhoon losses.

Declarations

Conflict of interest The authors have not disclosed any competing interests.

References

Ahmad I, Dar MA, Fenta A, Halefom A, Nega H, Andualem TG, Teshome A (2021) Spatial configuration of groundwater potential zones using OLS regression method. J Afr Earth Sci 177:104147. https://doi.org/10.1016/j.jafrearsci.2021.104147

Anselin L, Syabri I, Kho Y (2010) GeoDa: an introduction to spatial data analysis. Handbook of applied spatial analysis. Springer, pp 73–89

Cha EJ, Knutson TR, Lee T, Ying M, Nakaegawa T (2020) Third assessment on impacts of climate change on tropical cyclones in the Typhoon Committee Region-part II: future projections. Trop Cyclone Res Rev 9(2):75–86. https://doi.org/10.1016/j.tcrr.2020.04.005

Chen PY, Yang YH, Lei XT, Qian YZ (2009) Cause analysis and preliminary hazard estimate of typhoon disaster in China. J Nat Disasters 18(01):64–73. https://doi.org/10.3969/j.issn.1004-4574.2009.01.010

Chen WF, Duan YH, Lu Y, Fang JY, Shi XW, Ren FM (2017) Review on tropical cyclone risk assessment. J Catastrophol 32(4):146–152. https://doi.org/10.3969/j.issn.1000-811X.2017.04.025

Chen C, Lee T, Chang C, Lee J (2018) Assessing typhoon damages to Taiwan in the recent decade: return period analysis and loss prediction. Nat Hazards 91(2):759–783. https://doi.org/10.1007/s11069-017-3159-x

Cheng-Lin GU, Jian-Cheng K, Guo-Dong Y, Zhi-Wei C (2016) Spatial and temporal variability of northwest pacific tropical cyclone activity in a global warming scenario. J Trop Meteorol 22(S1):15–23. CNKI: SUN: RQXB.0.2016-S1-002. https://doi.org/10.16555/j.1006-8775.2016.S1.002

Corban C, Florczyk A, Freire S, Kemper T, Ehrlich D, Siragusa A, Pesaresi M (2017) Atlas of the human planet 2017: global exposure to natural hazards. http://repo.floodalliance.net/jspui/handle/44111/3706

Ding Y, Liu J, Chen S, Cheng X, Zheng Z (2020) Uniqueness of Lekima compared to tropical cyclones landed in the east coast of China during 1979–2019. Acta Oceanol Sin 39(8):121–124. https://doi.org/10.1007/s13131-020-1639-4

Esteban M, Valenzuela VP, Yun NY, Mikami T, Shibayama T, Matsumaru R, Takagi H, Thao ND, De Leon M, Oyama T (2015) Typhoon Haiyan 2013 evacuation preparations and awareness. Int J Sustain Future Hum Secur 3(1):37–45. https://doi.org/10.24910/jsustain/3.1/3745

Gao Y, Wang H, Liu GM, Sun XY, Fei XY, Wang PT, Lv TT, Xue ZS, He YW (2014) Risk assessment of tropical storm surges for coastal regions of China. J Geophys Res Atmos 119(9):5364–5376

Gettelman A, Bresch DN, Chen CC, Truesdale JE, Bacmeister JT (2018) Projections of future tropical cyclone damage with a high-resolution global climate model. Clim Change 146(3):575–585. https://doi.org/10.1007/s10584-017-1902-7

De Groeve T, Poljansek K, Ehrlich D (2013). Recording disaster losses. Recommendations for a European research. In: JRC scientific and policy reports. Joint Research Centre, European Commission. https://doi.org/10.2788/98653.

Gu XL, Chen YL, Qian YZ, Zhu JM, Jiang LL (2018) Typhoon disaster assessment and risk assessment based on hierarchical analysis method in Ningbo. J Trop Meteorol 34(4):489–498. https://doi.org/10.16032/j.issn.1004-4965.2018.04.006

Guo W, Zhou Q, Jia Y, Xu J (2020) Division of myocardial enzyme reference intervals in population aged 1 to < 18 years old based on Fisher's optimal segmentation method. Comput Math Methods Med. https://doi.org/10.1155/2020/2013148

Klawa M, Ulbrich U (2003) A model for the estimation of storm losses and the identification of severe winter storms in Germany. Nat Hazard 3(6):725–732. https://doi.org/10.5194/nhess-3-725-2003

Lei X, Zhou X (2012) Summary of retired typhoons in the Western North Pacific ocean. Trop Cyclone Res Rev 1(1):23–32. https://doi.org/10.6057/2012TCRR01.03

Lei XT, Chen PY, Yang YH, Qian YZ (2009) Characters and objective assessment of disasters caused by typhoons in China. Acta Meteorol Sin 67(05):875–883. https://doi.org/10.3321/j.issn:0577-6619.2009.05.018

Li CC, Li N, Du XH, Cheng XT, Wan JH (2016) The impact factors analysis of typhoon disasters in Fujian Province. China Flood Drought Manag 26(02):41–46. https://doi.org/10.3969/j.issn.1673-9264.2016.02.014

Liu FT, Xu EQ (2020) Spatio-temporal correlation analysis of typhoon characteristics and disaster assessment in Hainan Province. J Catastrophol 35(02):217–223. https://doi.org/10.3969/j.issn.1000-811X.2020.02.039

Lu XQ, Yu H, Ying M, Zhao BK, Zhang S, Lin LM, Bai LN, Wan RJ (2021) Western North Pacific tropical cyclone database created by the China meteorological administration. Adv Atmos Sci 38(4):690–699. https://doi.org/10.1007/s00376-020-0211-7

Meng F, Kang JC, Li WJ, Wu T, Wang TT, An Y (2007) Analysis and Evaluation of typhoon disasters in Shanghai in past 50 years. J Catastrophol. http://dx.chinadoi.cn/10.3969/j.issn.1000-811X.2007.04.016(04)

Nakamura R, Shibayama T, Esteban M, Iwamoto T (2016) Future typhoon and storm surges under different global warming scenarios: case study of typhoon Haiyan (2013). Nat Hazards 82(3):1645–1681. https://doi.org/10.1007/s11069-016-2259-3

Nerem RS, Beckley BD, Fasullo JT, Hamlington BD, Masters D, Mitchum GT (2018) Climate-change-driven accelerated sea-level rise detected in the altimeter era. Proc Natl Acad Sci 115(9):2022–2025. https://doi.org/10.1073/pnas.1717312115

Niu Y, Fang J, Chen R, Xia Z, Xu H (2020) Network modeling and dynamic mechanisms of multi-hazards—A case study of typhoon Mangkhut. Water 12(8):2198. https://doi.org/10.3390/w12082198

Park DR, Ho C, Chan JC, Ha K, Kim H, Kim J (2017) Asymmetric response of tropical cyclone activity to global warming over the North Atlantic and western North Pacific from CMIP5 model projections. Sci Rep 7(1):1–9. https://doi.org/10.1038/srep41354

Schmidt S, Kemfert C, Höppe P (2010) The impact of socio-economics and climate change on tropical cyclone losses in the USA. Reg Environ Change 10(1):13–26

Shao M, Dong YX, Lin CS (2020) Spatial and temporal evolution and drivers of ecosystem services in Chengdu–Chongqing urban agglomeration based on GWR model. J Beijing For Univ 42(11):118–129. https://doi.org/10.1217/j.1000-1522.20200217

Wang K, Yang Y, Reniers G, Huang Q (2021) A study into the spatiotemporal distribution of typhoon storm surge disasters in China. Nat Hazards 108(1):1237–1256

Webster PJ, Holland GJ, Curry JA, Chang H (2005) Changes in tropical cyclone number, duration, and intensity in a warming environment. Science 309(5742):1844–1846. https://doi.org/10.1126/science.1116448

Wu L, Wang R, Feng X (2018) Dominant role of the ocean mixed layer depth in the increased proportion of intense typhoons during 1980–2015. Earth's Future 6(11):1518–1527. https://doi.org/10.1029/2018EF000973

Wu JS, Zhao YH, Tian Y, Chen BK (2020) Evolution of typhoon disasters characteristics and non-structural disaster avoidance measures in the China coastal main functional area. Int J Disaster Risk Reduct 46:101490

Yang L, Cao C, Wu D, Qiu H, Lu M, Liu L (2018) Study on typhoon disaster loss and risk prediction and benefit assessment of disaster prevention and mitigation. Trop Cyclone Res Rev 7(4):237–246. https://doi.org/10.6057/2018TCRR04.05

Yin J, Yin Z, Xu S (2013) Composite risk assessment of typhoon-induced disaster for China's coastal area. Nat Hazards 69(3):1423–1434. https://doi.org/10.1007/s11069-013-0755-2

Ying MW, Zhang H, Yu X, Lu J, Feng Y, Fan Y, Zhu Y, Chen D (2014) An overview of the China meteorological administration tropical cyclone database. J Atmos Ocean Technol 31:287–301. https://doi.org/10.1175/JTECH-D-12-00119.1

Zhang Y, Fan G, He Y, Cao L (2017) Risk assessment of typhoon disaster for the Yangtze River Delta of China. Geomat Nat Hazards Risk 8(2):1580–1591

Zhang X, Nie J, Cheng C, Xu C, Zhou L, Shen S, Pei Y (2021) Natural and socioeconomic factors and their interactive effects on house collapse caused by typhoon mangkhut. Int J Disaster Risk Sci 12(1):121–130. https://doi.org/10.1007/s13753-020-00322-6

Zhi R, Zhang J, Bi J, Zhuang Z, Sai Q (2019) Characteristic analysis and prediction modeling of car-sharing user rental based on Fisher ordered clustering. IOP Conf Ser Mater Sci Eng 688:033019

Zhu J, Lu Y, Li GP, Ren FM (2017) Risk assessment of typhoon disasters in Fujian Province of each county. J Catastrophol 32(03):204–209. https://doi.org/10.3969/j.issn.1000-811X.2017.03.034

Zuzak CE, Goodenough C, Stanton M, Mowrer N, Ranalli D, Kealey J, Rozelle S (2021) National risk index technical documentation. Federal Emergency Management Agency, Washington, DC https://www.fema.gov/sites/default/files/documents/fema_national-risk-index_technical-documentation.pdf

Publisher's Note Springer Nature remains neutral with regard to jurisdictional claims in published maps and institutional affiliations.